Effects of Chemical Extraction Treatments on Nano-scale Mechanical Properties of the Wood Cell Wall

Shuang-Yan Zhang,[a] Bei-Hua Fei,[b,*] and Chuan-Gui Wang [a]

Chinese fir (*Cunninghamia lanceolata* (Lamb.) Hook) was subjected to chemical extraction treatments with sodium chlorite ($NaClO_2$) for delignification, as well as sodium hydroxide (NaOH) at various concentrations for extracting hemicelluloses gradually. Nanoindentation tests, X-Ray diffraction (XRD), and Fourier transform Raman (FT-Raman) spectroscopy studies revealed the changes in the mechanical properties and the nanostructure of the cell wall. The X-ray analysis indicated that delignification had only a moderate effect on the structure of the cell wall, while further alkali treatment led to major changes in the nanostructure. The nanoindentation tests showed that the indentation modulus and the hardness decreased after delignification and further alkali treatment, respectively. The indentation modulus of the cell wall with delignification decreased by 6.4% compared with the native cell wall, and the hardness decreased by 16.3%. After further alkali treatment, the indentation modulus and the hardness of the cell walls were 14.8% and 18.4% lower than that of the native cell walls, respectively. Additionally, the indentation modulus and the hardness of Chinese fir treated by NaOH decreased by 8.4%, and 2.1% in comparison with delignification, respectively. The results indicated that removal of hemicelluloses resulted in more damage to the mechanical properties of the cell wall compared with lignin.

Keywords: Extraction; Cell wall; Nanostructure; Nanoindentation; Nano-mechanical strength

Contact information: a: School of Forestry and Landscape Architecture, Anhui Agricultural University, Hefei, 230036, China; b: International Center for Bamboo and Rattan, No. 8, Futong Dong Dajie, Wangjing Area, Chaoyang District, Beijing, 100102, China;
** Corresponding author: feibenhua@icbr.ac.cn*

INTRODUCTION

With the increasing use of wood fibers as a raw material for producing "eco-friendly" composites in recent years, the study of the mechanical properties of wood fibers and cell walls has attracted increasing attention. The mechanical properties of wood fibers, especially nano-mechanical properties, might be of interest for the "fiber-related" industries, for example, pulp and paper, fiberboard, and might be of importance to serve for further and future material simulations. Cellulose, hemicelluloses, and lignin are the main chemical components of wood cell wall. The arrangement of the chemical components, their interactions, and the mechanical properties determine the mechanical properties of the cell walls. Thus, this study aimed at the investigation of nanoscale mechanical properties of the wood cell wall using nanoindentation to obtain a better understanding of how the chemical components affect the mechanical properties of the wood cell wall.

Nanoindentation, known as instrumented or depth-sensing indentation, is a well-established technique to characterize the mechanical properties of materials at very small

length scales (Eder *et al.* 2013). Wimmer *et al.* (1997) introduced nanoindentation in 1997 for the examination of wood cell wall mechanics. Since then, many authors have used this method in several fields of wood research, such as characterizing the adhesive bond effect on the cell wall properties in a defined area (Konnerth and Gindl 2006), examining the effects of forest management practices on wood micro-scale properties (Duchesne *et al*. 2011), wood property variations with cell wall characteristics (microfibril angle, cellulose, and lignin content) (Jungnikl *et al*. 2008), wood modification (Stanzl-Tschegg *et al.* 2009; Konnerth *et al*. 2010), creep behavior of lyocell fibers (Lee *et al*. 2007), and the effect of heat treatment on the mechanical properties of the cell wall (Zickler *et al*. 2006). It has been hypothesized that any change observed at the smallest scale should reflect, to some extent, a change in wood properties at a larger level (Vincent *et al.* 2014).

In this study, wood cell walls were treated with chemical extraction treatments. nanoindentation tests, FT-Raman, and X-ray diffraction were used to elucidate the relationship between the nanoindentation data and the cell wall structure.

EXPERIMENTAL

Materials

Material was taken from the adult wood of a 42-year-old Chinese fir (*Cunninghamia lanceolata* (Lamb.) Hook) grown in the Anhui Province of China. Samples measuring approximately 1 mm (tangential) × 1 mm (radial) × 5 mm (longitudinal), were cut from the mature latewood at breast height of the tree, as shown in Fig. 1. The samples were first extracted using alcohol-benzene solubility according to GB/T 2677.6 (1994). Then, the samples were delignified using an aqueous solution with a pH of 2.69, consisting of 150 mL of distilled water, 1.0 g of $NaClO_2$, and 2.0 mL of glacial acetic acid purchased from Nanjing Chemical Reagent Co., Ltd. (Nanjing, China) for 8 h, at 80 °C. On the delignified samples, a successive extraction of hemicelluloses was carried out by a treatment with 6%, 8%, and 10% of NaOH at 60 °C, for 2 h each (Nelson 1961). After all of the treatments, the samples were washed in deionized water and then stored in a refrigerator at 4 to 8 °C.

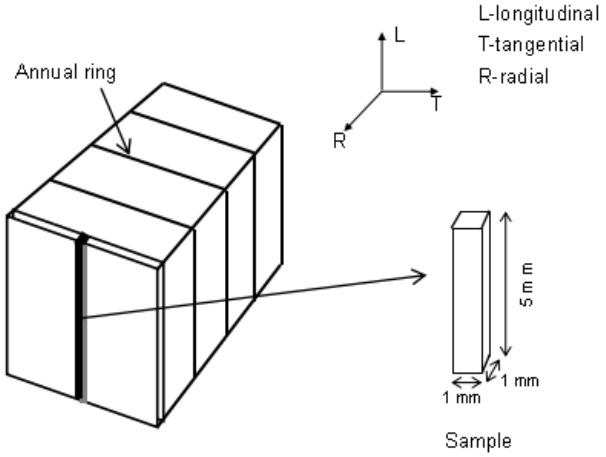

Fig. 1. Sample preparation

FT-Raman Spectroscopy

FT-Raman spectra were collected from the dried samples after the X-ray measurements. Three spectra per sample were measured, depending on the condition of the sample. A Nexus 670 spectrometer (Thermo Nicolet Co., USA) was used. The spectra were measured with a resolution of 4 cm^{-1}, from 4000 to 400 cm^{-1}, with 200 scans per measurement. The spectra were averaged and normalized using OMINIC software version 7.1 (Thermo Nicolet Corporation, USA). Only the relative changes in the averaged spectra were evaluated. Characteristic wavenumbers of the cell wall polymer bands that were used for evaluating the effects of the treatments are listed in Table 1.

Table 1. Assignment of Bands in the FT-Raman Spectrum of Cell Wall Polymers (Agarwal *et al.* 1997, 1999)

	Wavenumber (cm^{-1})	Band assignment
Lignin	1601	Aryl ring stretching, symmetric
	3065	Aromatic C-H stretch
Cellulose	1377	HCC, HCO, and HOC bending
	1456	HCH and HOC bending
	2895	CH and CH_2 stretching
Carbohydrates	1095	CC and CO stretching

XRD Measurements

X-Ray diffraction (XRD) measurements were performed to assess the crystalline properties of the dried sample cell walls using an X-Ray diffractometer (AV300, Panalytical Co., USA). The X-Ray generator was equipped with a copper tube operating at 40 kV and 200 mA, irradiating the sample with monochromatic Cu Kα radiation with a wavelength of 0.154 nm. The XRD spectra were acquired at room temperature over the 2θ angle range of 5° to 45°, at 0.05° intervals, with a measurement time of 1 s per 2θ interval. For each replicate sample, three spectra were considered.

According to the peak height method, developed by Segal *et al.* (1959), the XRD crystallinity index (C_rI) was calculated from the following height ratio,

$$C_r I(\%) = \frac{I_{002} - I_{am}}{I_{002}} \times 100 \quad (1)$$

where I_{002} is the reflection intensity of the 002 crystalline peak at 22° and I_{am} is the intensity at the minimum near 18° of the 2θ angle, which is between the 002 and the 101 peaks.

The average crystallite size was calculated from the Scherrer (1918) equation, with the method based on the width of the diffraction patterns obtained in the X-ray reflected crystalline region. The crystalline size D_{002} was determined using the diffraction pattern obtained from the 002 lattice planes of cellulose,

$$D_{002} = \frac{\kappa\lambda}{B_{002} COS\theta} \quad (2)$$

where κ is a constant (0.918), λ is the X-ray wavelength at 0.154 nm, B is the full-width, in radians, at half of the peak of the 002 reflection, and θ is the corresponding Bragg angle.

Nanoindentation Test

Chemically isolated samples were randomly selected for nanoindentation (Triboindenter, Hysitron, Minneapolis, MN) testing. Using an alternating vacuum-pressure treatment, the samples were embedded in a Spurr resin, which is composed of 5.0 g of cycloaliphatic epoxide resin, 3.0 g of polycyclodiepoxide, 13 g of nonenyl succinic anhydride, and 0.15 g of dimethylaminoethanol, and cured at 70 °C for 8 h (Zhu 1983). After the resin was cured, the cross-section of the samples was cut by an ultramicrotome (LKB-2188, RMC, USA) with a diamond knife, to obtain a very smooth surface for indenting. Quasi-static indentation tests were performed under environmental conditions, of 24 °C and 47% relative humidity (RH), in the cell wall of latewood. In a force-controlled mode, the indenter tip, which was a Berkovich-type triangular pyramid, was loaded to a peak force of 150 μN, at a loading rate of 30 μN/s. The hold time was 6 s. Figure 2 shows a light-microscope image of wood cells with indentations after nanoindentation testing. Figure 3 shows the loading history of a typical nanoindentation test. According to the method developed by Oliver and Pharr (1992), the indentation modulus and the hardness of materials can be calculated using Eqs. 3 and 4,

$$E = (1-\nu^2)\left(\frac{1}{E_r} - \frac{1-\nu_i^2}{E_i}\right)^{-1} \quad (3)$$

$$H = \frac{P_{\max}}{A(h_c)} \quad (4)$$

where E_i and ν_i are, respectively, the elastic modulus and the Poisson ratio of the tips. For the diamond tips, E_i is 1141 GPa and ν_i is 0.07. The E_r is called the reduced modulus, which is directly given by the instrument. The E and ν are, respectively, the elastic modulus and the Poisson ratio of the samples. The value 0.4 and 0.3 were adopted here as the longitudinal Poisson ratio of the softwood cell wall and Spurr resin, respectively (Jiang *et al.* 2004). H is the hardness of the samples. The variable P_{max} refers to the load measured at a maximum depth of penetration (h_c) in an indentation cycle, while $A(h_c)$ refers to the projected area of contact between the indenter and the sample at P_{max}.

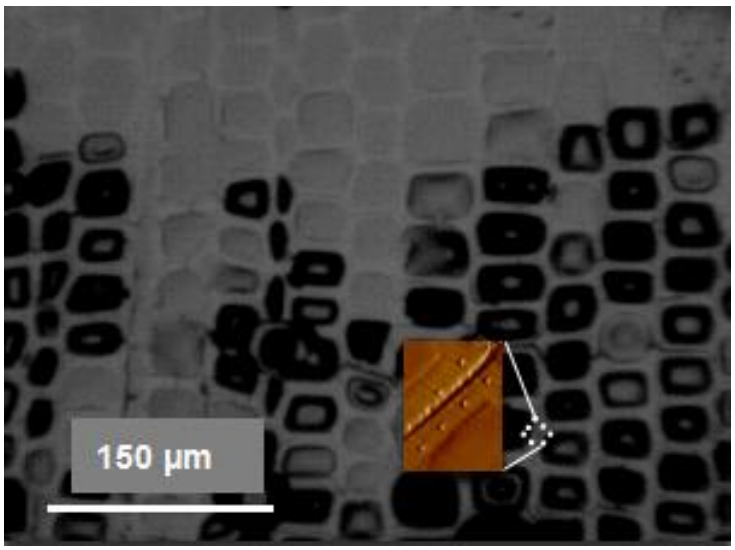

Fig. 2. Light-microscope image of Chinese fir and the scanning image after indentation

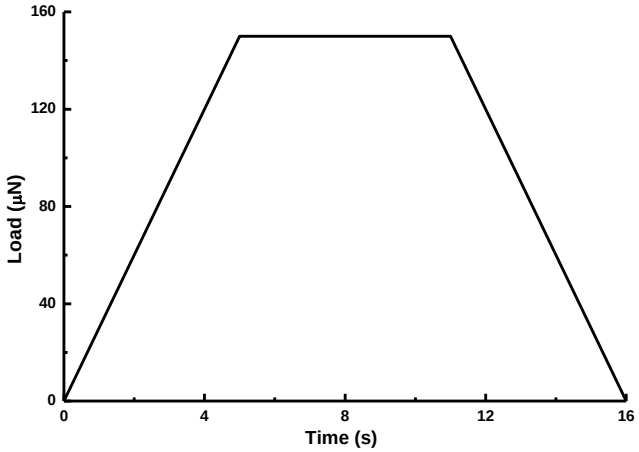

Fig. 3. Load-time curve of the cell wall performed in feedback force control mode

RESULTS AND DISCUSSION

FT-Raman Spectroscopy

The FT-Raman measurements were used to assess the effect of the treatments on the samples, which provided a good basis for a semi-quantitative interpretation of the cell wall chemical components. The FT-Raman spectra of the chemical extracted samples are shown in Fig. 4.

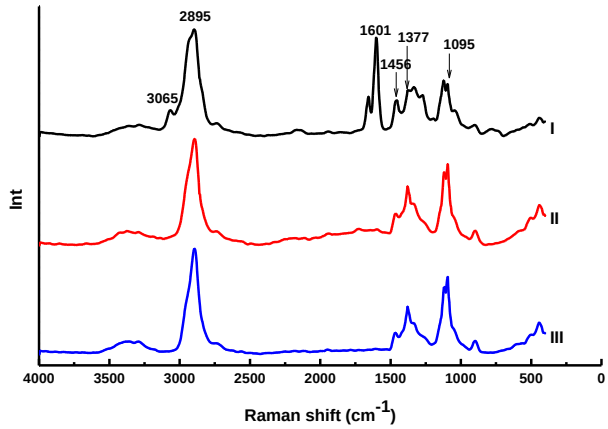

Fig. 4. The FT-Raman spectra: (I) native, (II) delignified, and (III) after subsequent extraction with 6%, 8%, and 10% NaOH for 2 h each

The lignin removal by the $NaClO_2$/glacial acetic acid can be observed by the disappearance of the bands at 1601 cm^{-1}, which are assigned to the aryl ring stretching and the aryl ring symmetric vibration, and 3065 cm^{-1}, which is assigned to the aromatic C-H stretch, as shown in Fig. 4 and listed in Table 1. This was similar to the studies of the lignin content determined by the amounts of acid-insoluble lignin, where the lignin content decreased to 0.4% after delignification. The peaks at 1377 and 2895 cm^{-1} are related to cellulose and showed a relative increase in samples treated by 6%, 8%, and 10% NaOH. This may be interpreted as a result of the hemicelluloses degradation. At this point, hemicelluloses degradation was affected to some extent, as can be seen from the shift of

the peak at 1456 cm^{-1} to near 1465 cm^{-1}, which indicated the formation of cellulose II, which is in agreement with the observation from the XRD measurements.

XRD Measurements

Typical X-ray diffractograms for the chemical extracted samples are shown in Fig. 5, and detailed crystalline properties are given in Table 2. No transition from cellulose I into cellulose II was observed after delignification. The peaks at 2θ = 12.1°, 20.4°, and 21.9° appeared after successive treatments with 6%, 8%, and 10% NaOH, as shown in Fig. 5 (Isogai *et al*. 1989; Fengel *et al*. 1995).

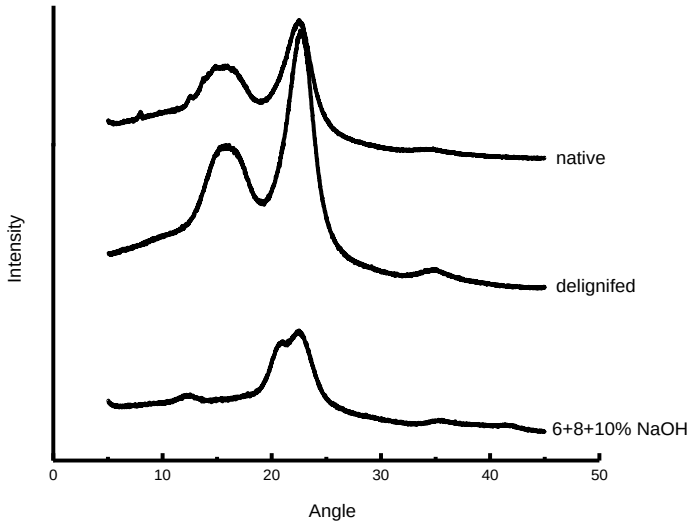

Fig. 5. X-ray diffractograms of samples: (I) native, (II) delignified, and (III) after subsequent extraction with 6%, 8%, and 10% NaOH for 2 h each

After delignification, the C_rI increased from 53% to 60.6%, as shown in Table 2. This can be attributed to the degradation of lignin, which reduced the amorphous fraction and consequently enriched the relative crystalline content. However, after the successive treatment with 6%, 8%, and 10% NaOH, the C_rI decreased from 53% to 50.8%. This suggests that the NaOH at 10% led to the molecular chain of cellulose crystalline becoming damaged (Yu *et al*. 2006). The crystallite thickness decreased from 2.189 to 2.116 nm after delignification, while it increased from 2.189 to 3.404 nm after subsequent extraction with NaOH. The apparent changes in the C_rI and the crystallite size may be due to a re-crystallization of the semi-crystalline cell wall component after the chemical extraction treatments.

Table 2. Crystallinity Index, C_rI, and Crystallite Thickness as Obtained by XRD Measurements on Samples after Chemical Extraction Treatments

Sample	C_rI (%)	Δ_{CrI} (%)	Crystallite Thickness (nm)	$\Delta_{thickness}$ (%)
Native	53.0	-	2.189	-
Delignified	60.6	14.3	2.116	-3.3
After subsequent extraction with 6%, 8%, and 10% of NaOH for 2 h each	50.8	-4.2	3.404	55.5

Nanoindentation Test

Indentation modulus of wood cell wall

The load-displacement curves from the nanoindentation experiments on the Chinese fir cell walls clearly indicated the elastic and plastic changes of the material after the extraction treatments. Figure 6 shows the typical load-displacement curves on the treated samples. The feedback force control mode ensures the actual peak load of all the indentations to be nearly equal to the set value of 150 μN, although they were performed on wood cell walls with chemical extraction treatments. The maximum depth of penetration increased with the degradation of the chemical components. Furthermore, the peak load of all the indentations remained constant during the holding segment, which ensured the reliability of the creep tests with nanoindentation.

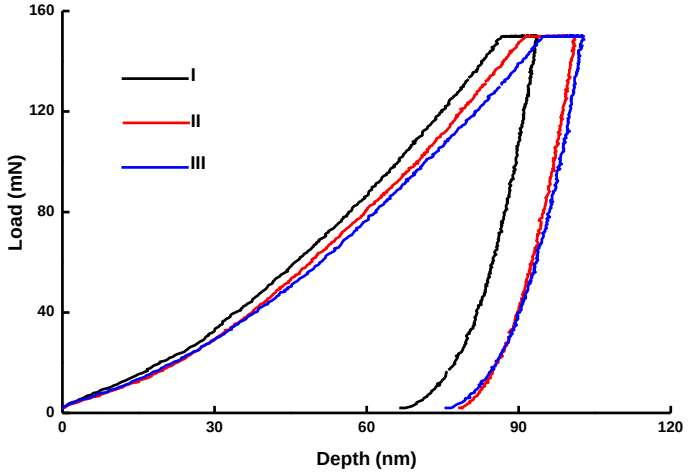

Fig. 6. Typical load-depth curves: (I) native, (II) delignified, and (III) after subsequent extraction with 6%, 8%, and 10% NaOH for 2 h each

The indentation moduli of the cell walls that were treated are displayed in Fig. 7. A decreasing trend in the indentation modulus was observed with the degradation of the chemical components. The quantitative analysis of the nanoindentation data revealed average indentation moduli of 20.3 ± 1.4, 19.0 ± 2.5, and 17.3 ± 2.6 for the S_2 wall of the Chinese Fir mature latewood for native, delignified, and alkali-treated samples. The indentation moduli of the cell wall after delignification and successive alkali treatment were 6.4% and 14.8% lower than that of the native cell wall, respectively. A similar trend in the mechanical properties with microtension was reported in a previous study (Zhang *et al*. 2013).

In Fig. 7, the indentation modulus of the Spurr resin, which was the embedding medium, was determined to be 4.1 GPa, as measured simultaneously with the wood cell wall measurements. The indentation modulus of the Spurr resin was far below that of the cell wall. Therefore, the presence of a small amount of Spurr resin in the cell wall is unlikely to affect the mechanical properties of the cell wall. Gindl *et al*. (2004) noted that the indentation modulus was directly proportional to the microfibril angle (MFA). The samples in this study were taken from the same site, where the MFAs were approximately 10°; therefore, it is safe to assume that the results were not due to MFA.

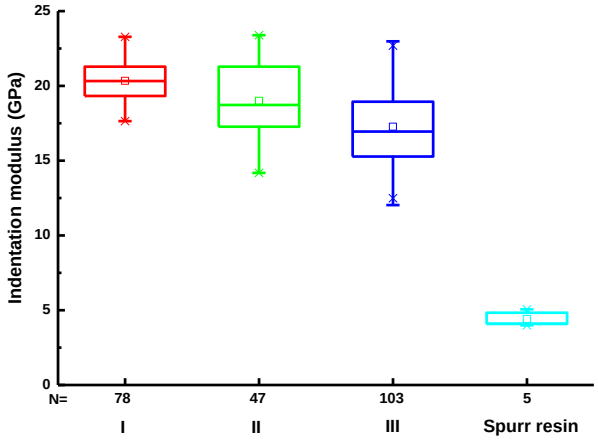

Fig. 7. Indentation modulus of cell walls: (I) native, (II) delignified, and (III) after subsequent extraction with 6%, 8%, and 10% NaOH for 2 h each

Bergander and Salmén (2002) summarized the values for the longitudinal Young's modulus of the wood cell wall components: 2.0 GPa for lignin, 7.0 GPa for hemicelluloses, and 167.5 GPa for cellulose. Thus, the degradation of lignin and hemicelluloses should not noticeably alter the stiffness of the composite cell wall. The removal of just the hemicelluloses caused more damage to the mechanical properties of the cell wall than the removal of the lignin. The hemicelluloses in the cell wall form a continuous network and serve as a transition between the cellulose microfibrils and the lignin regions. The degradation of hemicelluloses led to changes in the cell wall structure. As shown in Fig. 5, the cellulose crystal structure did not change after delignification; it was still cellulose I. After the extraction of hemicelluloses, a clear change in the cellulose crystal structure occurred, and peaks at 12.1°, 20.4°, and 21.9° appeared, indicating the formation of cellulose II (Isogai *et al.* 1989).

Hardness of wood cell wall

The hardness measured by nanoindentation is shown in Fig. 8. After the chemical extraction treatments, a clear decrease in the hardness was also observed. The average hardnesses obtained were 0.49 ± 0.04, 0.41 ± 0.04, and 0.40 ± 0.06 GPa for the native, delignified, and alkali-treated samples, respectively.

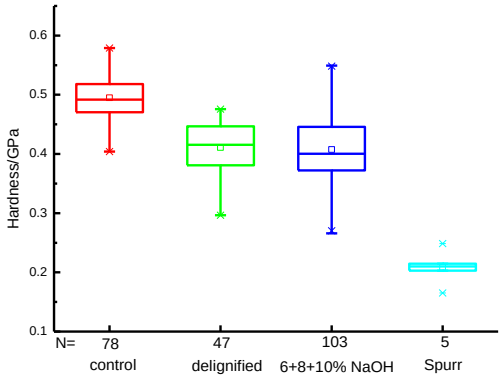

Fig. 8. Hardness of cell walls: (I) native, (II) delignified, and (III) after subsequent extraction with 6%, 8%, and 10% NaOH for 2 h each

In Fig. 8, the hardness of the Spurr resin, which was the embedding medium, was determined to be 0.21 GPa. Hardness is an important indicator of materials, representing the resistance to permanent plastic deformation. The hardness was observed to be reduced after the degradation of the matrix. After delignification, the hardness was 16.3% lower than that of the native cell walls. Compared with delignification, the hardness decreased by only 2.1% after further extraction with NaOH. This occurred because lignin has a comparably high hardness. The studies of Tze *et al.* (2007) and Gindl *et al*. (2002) also demonstrated that lignin may contribute to the hardness of the cell wall.

Creep properties of wood cell wall

Figure 9 shows the creep rate of wood cell walls, determined from nanoindentation. Compared with the native sample, the wood cell walls after delignification showed a minor increase in the creep rate. However, the creep rate of wood cell walls decreased with alkali treatment. Fioravanti *et al.* (2006) and Navi and Stanzl-Tschegg (2009) reported a similar result. This result showed that there was a lower viscoelasticity without the hemicelluloses compared with that of natural wood under constant climatic conditions. This may be the reason that the average size of the crystallites increased after the hemicelluloses extraction treatment, as shown in Table 2.

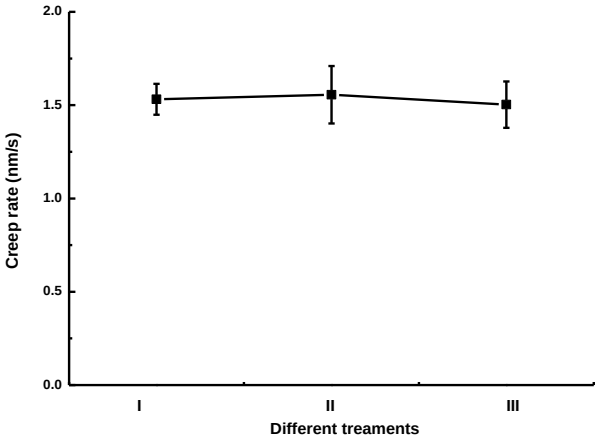

Fig. 9. Creep rate of cell walls: (I) native, (II) delignified, and (III) after subsequent extraction with 6%, 8%, and 10% NaOH for 2 h each

CONCLUSIONS

The mechanical properties and the crystalline cellulose structures of the wood cell walls with chemical extraction treatments all changed differently.

1. With the delignification treatment, the relative crystallinity increased, while the crystallite thickness decreased compared to that of the native cell walls. After the successive extraction treatment, the relative crystallinity was found to decrease while the crystallite thickness increased. The cellulose formation had changed after the successive extraction treatment with 6%, 8%, and 10% of NaOH.
2. The nanoindentation tests on the wood cell walls showed that the decreasing indentation modulus and hardness in samples that were chemically treated was

consistent with the degradation of lignin and hemicelluloses. After delignification, the indentation modulus of the wood cell walls decreased by 6.4%, compared to that of the native samples, and the hardness decreased by 16.3%. After further extraction treatments with NaOH, the indentation modulus and hardness of wood cell walls were obtained as 8.4% and 2.1% lower than that of cell walls after delignification, respectively. In addition, the wood cell walls without hemicelluloses had a lower viscoelasticity than the delignified cell walls under constant climatic conditions.

3. The removal of hemicelluloses caused more damage to the mechanical properties of the cell wall than the removal of lignin.

ACKNOWLEDGEMENTS

The authors are grateful for the support of the Department of Biomaterials of the International Center for Bamboo and Rattan, in Beijing, China. The authors would like to gratefully acknowledge the financial support from the Chinese National Natural Science Foundation (No. 31200436 and No. 31270591).

REFERENCES CITED

Agarwal, U. P. (1999). "An overview of Raman spectroscopy as applied to lignocellulosic materials," in: *Advances in Lignocellulosics Characterization*, D. Argyropoulos (ed.), TAPPI Press, pp. 201-225.

Agarwal, U. P., Ralph, S. A., and Atalla, R. H. (1997). "FT Raman spectroscopic study of softwood lignin," in: *Proc. 9th National Symposium, Wood Pulp. Chem.* pp. 8-10.

Bergander, A., and Salmén, L. (2002). "Cell wall properties and their effects on the mechanical properties of fibers," *J. Mater. Sci.* 37(1), 151-156.

Duchesne, I., Tong, T., Torquatos, L. P., Escobar, W. G., Bustos, C., Achim, A., Concha, K., and Cloutier, A. (2011). "Impact of spacing on modulus of elasticity and hardness of jack pine cell walls," in: *2011 Annual Meeting of the International Academy of Wood Science*, Stockholm, Sweden, July 03-06.

Eder, M., Arnould, O., Dunlop, J. W. C., Hornatowska, J., and Salmén, L. (2013). "Experimental micromechanical characterisation of wood cell walls," *Wood Sci. Technol.* 47(1), 163-182. DOI: 10.1007/s00226-012-0515-6

Fengel, D., Jakob, H., and Strobel, C. (1995). "Influence of the alkali concentration on the formation of cellulose-II-study by X-ray-diffraction and FTIR spectroscopy," *Holzforschung* 49(6), 505-511.

Fioravanti, M., Sodini, N., and Navi, P. (2006). "Investigation of the influence of hemicelluloses on time dependent behaviour of wood," in: *Proceedings of the International Conference on Integrated Approach to Wood Structure*, Behaviour and Application, Joint Meeting of ESWM and COST Action E35, Florence, Italy, pp.190-194.

GB/T 2677.6 (1994). "Fibrous raw material- Determination of solvent of extractives," China Standards Press, Beijing, China.

Gindl, W., Gupta, H. S., and Grunwald, C. (2002). " Lignification of spruce tracheid secondary cell walls related to longitudinal hardness and modulus of elasticity using nano-indentation," *Can. J. Bot.* 80(10), 1029-1033.

Gindl, W., Gupta, H. S., and Schoberl, T. (2004). "Mechanical properties of spruce wood cell walls by nanoindentation," *Appl. Phys. A-Mater.* 79(8), 2069-2074.

Isogai, A., Usuda, M., and Kato, T. (1989). "Solid state CP/MAS 13C NMR study of cellulose polymorphs," *Macromolecules* 22(7), 3168-3172.

Jungnikl, K., Koch, G., and Burgert, I. (2008). "A comprehensive analysis of the relation of cellulose microfibril orientation and lignin content in the S2 layer of different tissue types of spruce wood (*Picea abies* (L.) Karst)," *Holzforschung* 62(4), 475-480.

Jiang, Z. H., Yu, Y., Fei, B., and Ren, H. (2004). "Using nanoindentation technique to determine the longitudinal elastic modulus and hardness of tracheids secondary wall," *Scientia Silvae Sinicae* 40(2), 113-118.

Konnerth, J., and Gindl, W. (2006). "Mechanical characterization of wood-adhesive interphase cell walls by nanoindentation," *Holzforschung* 60(4), 429-433.

Konnerth, J., Eiser, M., and Jäger, A. (2010). "Macro- and micro- mechanical properties of red oak wood (*Quercus rubra* L.) treated with hemicellulases," *Holzforschung* 64(4), 447-453.

Lee, S. H., Wang, S. Q., and Pharr, G. M. (2007). "Mechanical properties and creep behavior of lyocell fibers by nanoindentation and nano-tensile testing," *Holzforschung* 61(3), 254-260.

Nelson, R. (1961). "The use of holocellulose to study cellulose supermolecular structure," *J. Polym. Sci.* 51(155), 27-58.

Navi, P., and Stanzl-Tschegg, S. (2009). "Micromechanics of creep and relaxation of wood: A review," *Holzforschung* 63(2), 186-195.

Oliver, W. C., and Pharr, G. M. (1992). "An improved technique for determining hardness and elastic modulus using load and displacement sensing indentation experiments," *J. Mater. Res.* 7(6), 1564-1583.

Stanzl-Tschegg, S., Beikircher, W., and Loidl, D. (2009). "Comparison of mechanical properties of thermally modified wood at growth ring and cell wall level by means of instrumented indentation test," *Holzforschung* 63(4), 443-448.

Segal, L., Creely, J. J., Martin, A. E., and Conrad, C. M. (1959). "An empirical method for estimating the degree of crystallinity of native cellulose using the X-ray diffractometer," *Text Res. J.* 29(10), 786-794.

Tze, W. T. Y., Wang, S., and Rials, T. G. (2007). "Nanoindentation of wood cell walls: Continuous stiffness and hardness measurements," *Compos. Part A-Appl. S.* 38(3), 945-953.

Vincent, M., Tong, Q. J., Terziev, N., Daniel, G., Bustos, C., Escobar, W. G., and Duchesne, I. (2014). "A comparison of nanoindentation cell wall hardness and Brinell wood hardness in jack pine (*Pinus banksiana* Lamb.)," *Wood Sci. Technol.* 48(1), 7-22. DOI: 10.1007/s00226-013-0580-5

Wimmer, R., Lucas, B. N., and Tsui, T. Y. (1997). "Longitudinal hardness and Young's modulus of spruce tracheid secondary walls using nanoindentation technique," *Wood Sci. Technol.* 31(2), 131-141.

Yu, C. H., Feng, X. X., Jia, C. L., and Chen, J. Y. (2006). "Effect of high temperature degumming of hemp on its composition and structure," *J. Text. Res.* 27(10), 80-83.

Zhu, L. X. (1983). *Electron Microscopy in Biology*, PeKing University Press, Beijing, China.

Zickler, G. A., Schoberl, T., and Paris, O. (2006). "Mechanical properties of pyrolyzed wood: A nanoindentation study," *Philos. Mag.* 86(10), 1373-1386.

Zhang, S. Y., Wang, C. G., Fei, B. H., Yu, Y., Cheng, H. T., and Tian, G. L. (2013). "Mechanical function of lignin and hemicelluloses in wood cell wall revealed with microtension of single wood fiber," *BioResources* 8(2), 2376-2385. DOI: 10.15376/biores.8.2.2376-2385

Article submitted: May 10, 2016; Peer review completed: June 17, 2016; Revised version received and accepted: July 10, 2016; Published: July 15, 2016.
DOI: 10.15376/biores.11.3.7365-7376